HOKKAIDO UNIVERSITY

Title	In situ Real-time Monitoring of Electrochemical Ag Deposition on a Reconstructed Au(111) Surface Studied by Scanning Tunneling Microscopy
Author(s)	Takakusagi, Satoru; Kitamura, Ken; Uosaki, Kohei
Citation	Journal of Physical Chemistry C, 112(8), 3073-3077 https://doi.org/10.1021/jp709916m
Issue Date	2008-02-28
Doc URL	https://hdl.handle.net/2115/50215
Type	journal article
File Information	JPCC112-8_3073-3077.pdf

Hokkaido University Collection of Scholarly and Academic Papers : HUSCAP

In situ Real-time Monitoring of Electrochemical Ag Deposition on a Reconstructed Au(111) Surface Studied by Scanning Tunneling Microscopy

Satoru Takakusagi, Ken Kitamura, and Kohei Uosaki*

Physical Chemistry Laboratory, Division of Chemistry, Graduate School of Science, Hokkaido University, Sapporo 060-0810, Japan

Received: October 11, 2007; In Final Form: November 18, 2007

Electrochemical deposition of Ag on a $23 \times \sqrt{3}$ reconstructed surface of Au(111) electrode at various potentials was followed by scanning tunneling microscopy (STM) in situ in real time. At −0.2 V (vs Ag/AgCl), line shaped Ag deposits with the height of 0.46 ± 0.03 nm, which is equivalent to 2 atomic height, were observed. The center of each Ag line was located in the hcp domain of the reconstructed structure. They then grew two-dimensionally so that the other regions, i.e., bridge and fcc domains, of the reconstructed Au surface were gradually covered with the Ag bilayer. As the deposition proceeded, another Ag layer started to nucleate and grow on the Ag bilayer. This layer was one atomic height and grew not linearly but two-dimensionally from the beginning. At 0.3 V, the monatomic layer of Ag was formed preferentially in the hcp domain and the Ag growth stopped at ca. 1 ML. The potential dependent stabilities of the deposited bi- and mono-atomic Ag layers were confirmed by the potential step measurements. The structural conversion from the bi- to mono-atomic layer of Ag was observed when the potential was stepped from −0.2 to +0.3 V. At 0 V, an intermediate potential, both the bi- and mono-atomic Ag layers were observed at the initial stage of Ag deposition. These results revealed that the biatomic Ag layer was more favored at more negative potentials in the range of −0.2 to +0.3 V. The growth mode of the potentiostatic electrochemical deposition of Ag on the reconstructed Au (111) electrode surface observed in this study is quite different from those previously reported for the electrochemical deposition on the reconstruction-lifted Au(111) electrode surface and deposition under ultrahigh vacuum (UHV) condition on the reconstructed Au(111) surface, showing the importance of structure of substrate surface and electrode potential on the growth mode.

1. Introduction

Silver deposition on Au(111) has been the subject of a number of studies because it is a good example of metal deposition where the interaction between a metal deposit and a substrate is very strong and the lattice misfit between the deposit and the substrate is negligible.[1−21] The deposition processes have been studied both in ultrahigh vacuum (UHV)[17−21] and electrochemical environments[1−16] by a wide variety of techniques, including scanning tunneling microscopy (STM),[1,2,5,8,9,14,16,17−21] atomic force microscopy (AFM),[3,4,6] second harmonic generation (SHG) spectroscopy,[13] quartz crystal microbalance (QCM),[7] ultra-violet photoelectron spectroscopy (UPS),[19,21] X-ray diffraction,[11,12] and extended X-ray absorption fine structure (EXAFS).[10] In the electrochemical deposition, underpotential deposition (UPD) has received special attention and the structure of adsorbates including both metal and anion and its dependence on the potential and electrolyte composition have been investigated.[2−6] For the UPD, formation of homogeneous Ag layer of various coverage up to two monolayer depending on the electrode potential has been reported.[14,15] Far fewer studies on the overpotential deposition (OPD) of Ag on Au(111) have been reported.[9,14] For example, a layer-by-layer growth was observed during the initial stage up to 10 monolayers at low overpotentials.[14] In almost all the cases, both UPD and OPD, the Au(111) electrode was initially kept at a potential much more positive than the Ag deposition potential and then scanned negatively or stepped to the potential more negative than the Ag deposition potential. The initial potential is actually positive enough to lift the reconstruction of Au(111) surface, and therefore, Ag deposition usually takes place on the (1×1) surface of Au(111).

Metal deposition on a reconstructed Au(111) surface, where uniformly spaced inhomogeneous sites are present, should be interesting because it can offer a unique method for the preparation of self-organized nanosized metal pattern. The influence of the Au(111) reconstruction on electrochemical deposition processes has been already shown in a number of systems. In the case of electrodeposition of Cd, regularly arranged arrays of Cd clusters were formed as a result of specific nucleation at the "elbow sites" of the reconstructed Au(111) surface.[22] Pb,[23] Co,[24] and Au−Cd alloy[25] have been found to electrodeposit selectively in the hcp area. Selective decoration of the fcc area was also reported for Ru deposition.[26] No reports of Ag electrodeposition on a reconstructed Au(111) surface have been published, however, due to the relatively positive reversible potential for Ag deposition. In UHV, line shaped Ag deposits of monatomic height were preferentially formed in the hcp area of the reconstructed Au(111) surface at submonolayer coverage, reflecting the morphology of the substrate surface.[17,21]

In the present study, the potentiostatic electrochemical deposition of Ag on a $23 \times \sqrt{3}$ reconstructed Au(111) surface at various potentials was investigated in situ in real time using electrochemical STM. After injecting a solution containing Ag_2SO_4 into the STM cell filled with H_2SO_4 at −0.2 V (vs

* To whom correspondence should be addressed. Phone: +81-11-706-3128. Fax: +81-11-706-3440. E-mail: uosaki@pcl.sci.hokudai.ac.jp.

10.1021/jp709916m CCC: $40.75 © 2008 American Chemical Society
Published on Web 02/06/2008

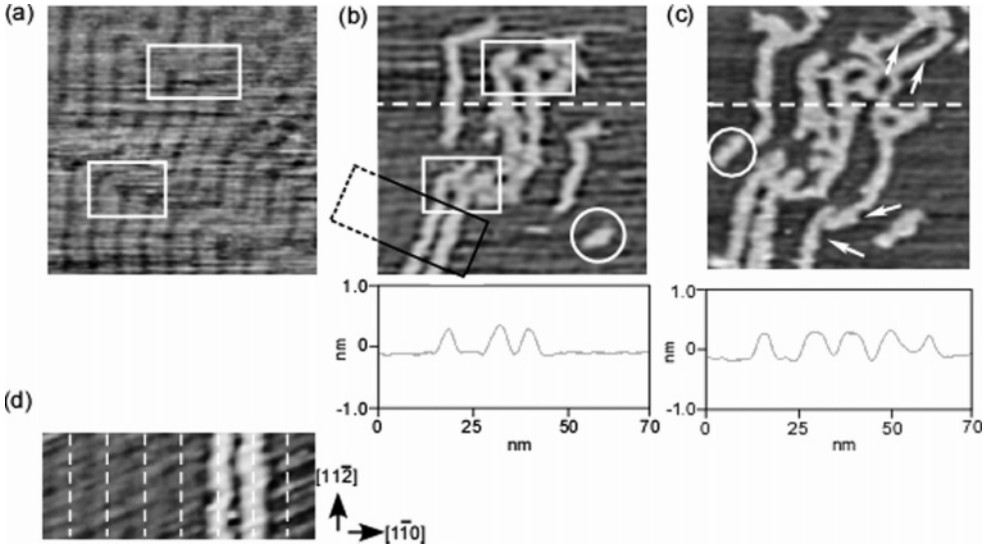

Figure 1. In situ STM images (70 × 70 nm^2) of Au(111) at −0.2 V (vs Ag/AgCl) in 50 mM H_2SO_4 (a) before and (b) 3 min and (c) 30 min after the addition of 2 μL of 1 mM Ag_2SO_4 + 50 mM H_2SO_4. (d) Enlarged in situ STM image (17.5 × 44.5 nm^2) of the bottom left corner of (b) as indicated by a black square. The concentration of Ag^+ in the cell was ca. 2 μM after the addition of the Ag_2SO_4 solution. E_{tip} = 0.35 V, I_{tip} = 3.0 nA.

Ag/AgCl), formation of line shaped Ag deposits of 2 atomic height along the herringbone reconstruction structure of Au(111) was observed followed by two-dimensional growth of the Ag bilayer to cover the other regions of the Au surface. Further deposition of Ag proceeded by the nucleation and isotropic two-dimensional growth of Ag monolayer on the Ag bilayer, indicating that the growth of the third Ag layer was not affected by the original reconstructed structure. In contrast, only the monatomic Ag layer was deposited along the herringbone reconstruction and the Ag did not grow over ca. 1 ML at +0.3 V. The potential dependent stabilities of bi- and mono-atomic Ag layer on the reconstructed Au(111) surface were confirmed as the conversion from bi- to mono-atomic layer was observed by stepping the potential from −0.2 to +0.3 V. At 0 V, an intermediate potential, both the bi- and mono-atomic layers of Ag were observed.

2. Experimental Section

2.1. Materials. A (111) facet on a single crystal bead of Au, which was prepared by the Clavilier's method,[27] was used as a substrate in the STM measurements. Electrolyte solutions were prepared using H_2SO_4 (Suprapure reagent grade, Wako Pure Chemicals), Ag_2SO_4 (Reagent grade, Wako Pure Chemicals), and Milli-Q water.

2.2. Electrochemical STM Measurements. In situ electrochemical STM measurements were carried out using a home-made electrochemical STM cell, which can accommodate the single-crystal electrode. STM images were recorded in a constant current mode using a NanoScope E (Digital Instruments). An Au/AuO_x and a platinum wire were used as a quasi-reference and a counter electrode, respectively. The electrolyte solution was deaerated by passing purified argon gas for at least 20 min before being introduced into the STM cell. Electrochemical potentials of the Au(111) substrate and STM tip (E_{tip}) were independently controlled by a bipotentiostat (Digital Instruments). All potentials were quoted vs Ag/AgCl in the present study. STM tips were mechanically cut Pt/Ir wire (80/20, φ = 0.3 mm) insulated with Apiezon wax. The single-crystal electrode was annealed with hydrogen flame just before the measurements and was mounted to the STM cell after cooling in air. A 50 mM H_2SO_4 solution was then introduced into the cell while controlling the electrode potential at a preset value.

3. Results and Discussion

3.1. Deposition at −0.2 V. *3.1.1. Nucleation and Submonolayer Growth.* Figure 1(a) shows a typical STM image of Au(111) surface in 50 mM H_2SO_4 measured at −0.2 V (vs Ag/AgCl). A characteristic feature of a series of zigzag pairs of double lines, a well-known herringbone structure of 23 × $\sqrt{3}$ reconstructed surface, was observed, although the double lines were not clearly resolved due to the insufficient resolution.

After the confirmation of the presence of the reconstructed phase, 2 μL of 1 mM Ag_2SO_4 + 50 mM H_2SO_4 solution was added to the STM cell so that the final concentration of Ag^+ became ca. 2 μM. Since the reversible potential for Ag/Ag^+ in 2 μM Ag^+ solution is calculated to be 0.26 V vs Ag/AgCl, −0.2 V is in OPD region. The STM images were sequentially captured at the same region of the Figure 1(a). Figure 1(b) and (c) are the STM images obtained at 3 and 30 min, respectively, after the solution containing Ag_2SO_4 was added to the cell. Shape of the deposits is totally different from that usually observed for Ag deposition on Au(111) where reconstruction has been lifted. While isotropical two-dimensional growth is usually observed at a Au(111)-(1 × 1) surface,[1,2,8,9,14,16] deposits observed on the reconstructed surface are in line shape, reflecting the shape of the herringbone structure of the Au(111) surface as shown in Figures 1(b) and (c). The reconstructed phase was remained to be clearly observed on the Au surface which was not covered with Ag deposits. Nucleation of the Ag islands seemed to take place at the hcp region located at the defect sites such as the bending point of the double lines of the reconstruction, which is often called "elbow site", as indicated by white circles in Figures 1(b) and (c) suggesting this site is very reactive. The Ag lines seemed to be interconnected preferentially also at the elbow sites as marked by the white rectangles in Figures 1(a) and (b) because of the high density of nuclei at these sites. The comparison of Figures 1(b) and (c) shows the growth of the chain with the deposition time as indicated by white arrows in Figure 1(c). The width of each Ag line also slightly increased. This is confirmed by a cross sectional analysis of the Ag deposits along the dotted lines in

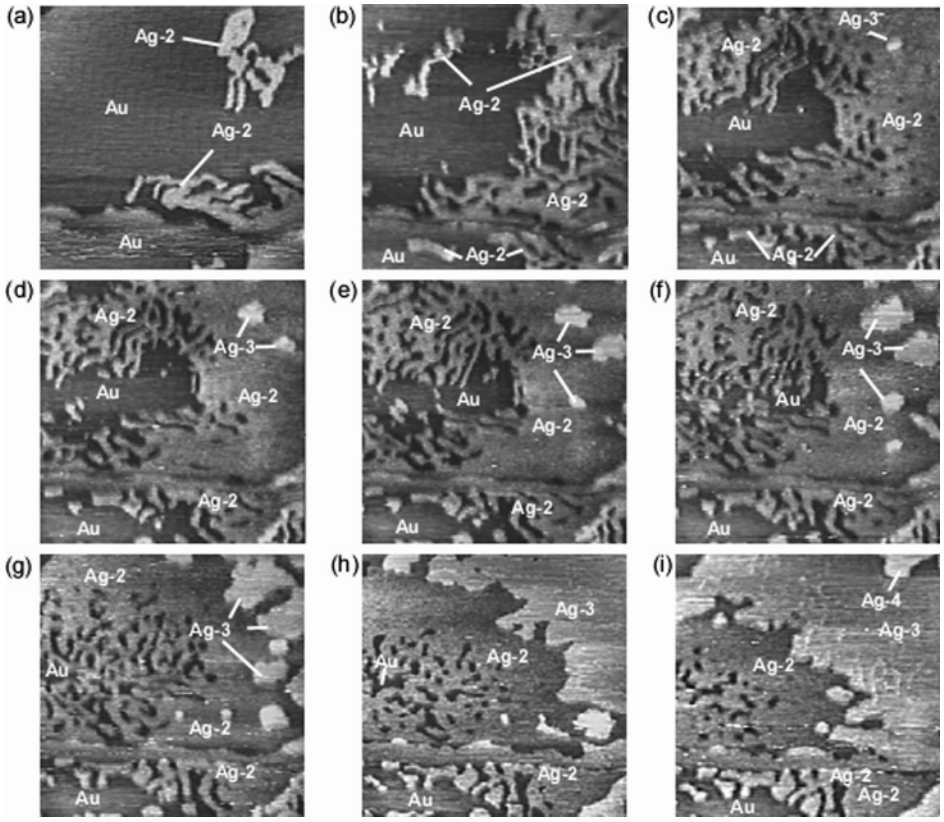

Figure 2. Sequentially obtained in situ STM images (150 × 150 nm^2) of the reconstructed Au(111) surface (a) 20 min, (b) 75 min, (c) 112 min, (d) 135 min, (e) 142 min, (f) 150 min, (g) 168 min, (h) 218 min, and (i) 260 min after the addition of 8 μL of 10 mM Ag_2SO_4 + 50 mM H_2SO_4 solution while keeping the electrode potential at −0.2 V (vs Ag/AgCl) in 50 mM H_2SO_4. 8 μL of 10 mM Ag_2SO_4 + 50 mM H_2SO_4 solution was further added after recording the STM image of (b). The concentration of Ag^+ was ∼80 and ∼160 μM after the first and second addition, respectively, of the Ag_2SO_4solution. E_{tip} = 0.55 V, I_{tip} = 3.0 nA.

the STM images of Figures 1(b) and (c). The line profiles also revealed that their height was 0.46 ± 0.03 nm, which is equivalent to 2 atomic height of Ag. Figure 1(d) is the magnified image of the black rectangular part of Figure 1(b), showing two parallel lines of Ag deposits. The dotted lines in this figure show the center of the paired lines of the Au reconstruction structure that is along the hcp region. It is clear that the center of each Ag line is located in the hcp domain, showing the preferential nucleation and growth of the Ag in the hcp region.

The slight increase of the line width of the Ag deposits with deposition time shown in Figures 1(b) and (c), indicate that the Ag deposits also grew along the <$1\bar{1}0$> directions but with a much slower rate. Ag deposits on a reconstructed Au(111) surface in UHV environment at submonolayer coverage show a similar line pattern with preferential growth on the narrower (presumably hcp) hollow-site regions.[17] These results show that the interaction of Ag seems to be stronger with the hcp region of the Au(111) reconstruction than with other regions. The selective decoration of the hcp area can be explained by considering heterogeneity in the adsorption energy and/or diffusion barrier for Ag atoms, which are relatively large in the hcp area, resulting in local trapping and subsequent nucleation of Ag deposits at these sites. At least two possibilities should be considered for the origin of the heterogeneity. One is the stacking effect and the other is the difference in local strain of the reconstructed Au(111) surface. Monatomic Co layer, which was preferentially deposited in the hcp region, was suggested to be energetically stabilized (larger adsorption energy) by adopting an hcp registry with the first two gold atomic planes so as to build a sort of "$CoAu_2$ thin hcp layer" (Co is an hcp-stacked metal).[24] Although bulk Ag is a fcc-stacked metal, the stabilization in the hcp region might be possible because Ru, which adopts hcp stacking in bulk metal, was found to be deposited selectively in the fcc region of the reconstructed Au-(111) surface.[26] As far as local strain is concerned, it has been reported that the in-plane surface nearest-neighbor atomic distance is different by ca. 2% between the hcp and fcc regions in the framework of the tight-binding second moment approximation.[28] This indicates that the degree of lattice mismatch between the deposited Ag and substrate Au in the hcp region should be different from that in the fcc region and such a difference causes local strain. Further investigation, particularly theoretical treatment, is necessary to reveal the origin for the selective deposition of Ag atoms in the hcp region.

It must be noted here that the Ag lines observed in UHV condition were of monatomic height while those observed in the present study were of biatomic height. These results clearly show the unique nature of the electrochemical deposition where electrochemical potential and electrolyte solution play important roles.

3.1.2. Multilayer Growth. The deposition process up to higher coverage was investigated in a solution of higher Ag^+ concentration where the deposition rate is higher. Figure 2 shows sequentially obtained STM images of the reconstructed Au(111) surface while keeping the potential at −0.2 V (vs Ag/AgCl) in 50 mM H_2SO_4 after 8 μL of 10 mM Ag_2SO_4 + 50 mM H_2SO_4 solution was added to the STM cell. The concentration of Ag^+ in the cell was ca. 80 μM after the addition of the Ag_2SO_4 solution. Ag deposits of ca. 0.47 nm, i.e., biatomic height, were observed 20 min after the addition of the Ag_2SO_4 solution indicated as Ag-2 in Figure 2(a). They grew two-dimensionally as the deposition proceeded with the characteristic feature

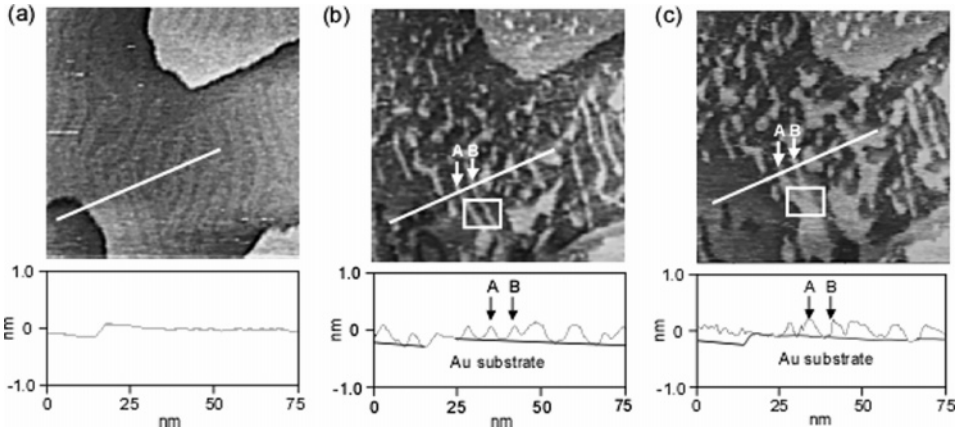

Figure 3. In situ STM images (75 × 75 nm^2) of the reconstructed Au(111) surface at +0.3 V in 50 mM H_2SO_4 (a) before, (b) 24 min, and (c) 29 min after the addition of 2 μL of 1 mM Ag_2SO_4 + 50 mM H_2SO_4. The concentration of Ag^+ in the cell was ca. 2 μM after the injection of the Ag_2SO_4 solution. E_{tip} = 0.55 V, I_{tip} = 3.0 nA.

reflecting the morphology of the underlying substrate (Figure 2(b)), confirming the results shown in Figure 1.

After capturing Figure 2(b), 8 μL of 10 mM Ag_2SO_4 + 50 mM H_2SO_4 solution was added again so that the concentration of Ag^+ in the cell became ca. 160 μM. Nucleation of another layer of Ag on the bilayer was observed at the upper right portion of Figure 2(c) indicated as Ag-3. This layer was of monatomic height and was not in line shape but grew rather isotropically as shown in Figures 2(d)−(g). Monatomic Ag islands grew and coalesced each other, and then formed a layer as shown in Figures 2(h) and (i). Formation of the fourth layer marked as Ag-4 was also seen at the upper right portion of Figure 2(i).

These experimental results can be qualitatively explained as follows. After preferential deposition of the biatomic Ag layer in the hcp region, the bilayer grew two-dimensionally covering the other regions such as bridge and fcc. When the Au surface was covered with a certain amount of Ag adatoms so that the Ag domains exceeded a critical size, it became unfavorable to maintain the reconstructed structure. The excess (4%) Au atoms might diffuse on the surface and might be incorporated into the Ag bilayer. After deposition of the third layer, diffusion and incorporation into the third layer also become possible as segregation of a small number of Au atoms in the Ag/Au(111) interface at room temperature has been reported.[29]

3.2. Deposition at +0.3 V. Figure 3(a) shows a typical STM image of Au(111) surface measured at +0.3 V in 50 mM H_2SO_4, confirming that the herringbone structure of 23 × $\sqrt{3}$ reconstructed surface was maintained at this potential.

Figures 3(b) and (c) show the STM images, which were acquired at 24 and 29 min, respectively, after injection of 2 μL of a solution containing 1 mM Ag_2SO_4 and 50 mM H_2SO_4. The concentration of Ag^+ in the cell was ca. 2 μM after the injection. In Figure 3(b), line shaped Ag deposits were observed on the terrace surface (for example see the white arrows indicated as A and B). The contrast of the substrate Au(111) reconstruction in the STM image was rather vague after Ag deposition, although it was clearly observed at −0.2 V (Figure 1). The careful analysis of Figures 3(a) and (b) suggests that the center of each Ag line was located in the hcp domain. The deposited Ag grew two-dimensionally with time, and the other regions were also covered with the Ag layer as shown in the white rectangles in Figures 3(b) and (c). The line profiles along the white lines in the STM images of Figures 3(b) and (c), revealed that the height of the deposited Ag was monatomic (0.23 ±0.03 nm), which is in contrast to the result at −0.2 V

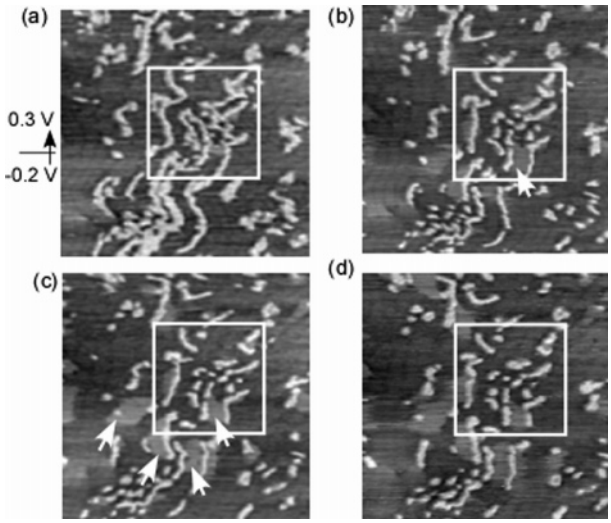

Figure 4. In situ STM images (150 × 150 nm^2) of the structural conversion of the biatomic Ag layers to the monatomic ones induced by the potential step from −0.2 V to +0.3 V. The potential was stepped at the middle of (a), (b)−(d) were acquired 2, 4, and 9 min, respectively, after the potential step. The concentration of Ag^+ in the cell was ca. 2 μM. E_{tip} = 0.55 V, I_{tip} = 3.0 nA.

where the biatomic layer was observed. This should be related with the fact that the applied potential was more positive than the reversible potential for Ag/Ag^+ (∼ +0.26 V) by +0.04 V, i.e., in UPD region where formation of a uniform monolayer of Ag on Au(111)-(1 × 1) surface has been reported.[14,15] The growth actually stopped at ca. 1 ML under the present condition.

3.3. Effect of Electrode Potential on Formation and Stability of Bi- and Mono-atomic Ag Layers. The results obtained in the previous section showed that although the nucleation and subsequent growth of Ag at −0.2 and +0.3 V were essentially the same, the heights of the Ag deposits were different. Since the structures of the underlying reconstructed surfaces of Au(111) at +0.3 and −0.2 V were the same, electrochemical potential should be a controlling factor for the formation of bi- and mono-atomic Ag layers as mentioned before.

Figure 4 is sequentially obtained STM images of the Au(111) electrode surface when the electrode potential was stepped from −0.2 to +0.3 V after the electrode potential was kept at −0.2 V for 30 min in a solution containing ca. 2 μM Ag_2SO_4 and 50 mM H_2SO_4. Before the potential step (the bottom part of Figure 4(a)), line shaped Ag deposits of biatomic

height were present on the reconstructed Au(111) surface. The potential was stepped at the middle of Figure 4(a), and Figures 4(b)−(d) were acquired 2, 4, and 9 min, respectively, after the potential step. The white squares indicate the same area. The Ag deposits of biatomic height disappeared with time and the area of another layer with medium STM contrast (white arrows) increased with time. The height of the newly formed layer was monatomic. The growth of the monatomic islands seemed to start from the biatomic Ag layer. The total Ag coverage, which was defined as {2 × (area of biatomic Ag layer) + (area of monatomic Ag layer)}/(total area of Au), was found to decrease immediately after the potential step from 0.60 ML (Figure 4(a)) to 0.38 ML (Figure 4(b)). The decrease was probably due to dissolution of a part of the biatomic Ag layers since the potential was stepped from more negative (OPD region) to more positive (UPD region) than the reversible potential of Ag/Ag^+ (∼+0.26 V). After the initial decrease, the total coverage was almost constant. These results show that after the initial dissolution, the biatomic Ag layer was gradually converted to the monatomic layer.

Ag deposition at an intermediate potential, 0 V, revealed that the preferential nucleation and growth of Ag in the hcp domain, resulting in a line shape, took place at this potential, but both the bi- and mono-atomic Ag layers were observed on the surface.

Thus, for the initial stage of Ag deposition on the reconstructed Au(111) surface, the more negative the deposition potential in the range of −0.2 to +0.3 V, the more favored the formation of the biatomic Ag layer than that of the monatomic Ag layer. This should be related with the fact that in the ordinary UPD process of Ag on Au(111), in which the potential was gradually swept in the negative direction, there exist the potential regions where the uniform monolayer and the bilayer of Ag are formed.[14,15] The observation of the monatomic Ag deposition at +0.3 V is well understood since the applied potential is in the UPD region where formation of Ag monolayer is reported. Further experimental and theoretical studies are required to reveal the origin of the potential dependent stability of bi- and mono-atomic Ag layers on the reconstructed Au(111) surface.

4. Conclusion

Electrodeposition of Ag on a reconstructed Au(111) surface at various potentials was followed by in situ STM in real time. At −0.2 V (vs Ag/AgCl), Ag of biatomic height was nucleated on the faulted hcp region of the reconstruction and grew preferentially along the hcp lines (the $<1\bar{1}2>$ directions), resulted in a line shape. The growth along the perpendicular directions (the $<\bar{1}10>$ directions) also proceeded but at a much slower rate and eventually covered the Au surface with the Ag bilayer. As the deposition proceeded, another Ag layer of monatomic height was nucleated on the bilayer and grew two-dimensionally, followed by coalescence of these monatomic Ag islands to form a third layer. Monatomic Ag layer was preferentially deposited in the hcp domain and the Ag growth stopped at ca. 1ML at 0.3 V. The potential dependent formation of the bi- and mono-atomic Ag layer on the reconstructed Au(111) surface was also confirmed by the structural conversion from the bi- to mono-atomic Ag layer when the electrode potential was stepped from −0.2 V to +0.3 V. At an intermediate potential, 0V, both the bi- and mono-atomic Ag layers were observed. These results show that formation of the biatomic Ag layer was more favored at more negative potentials in the range of −0.2 to +0.3 V The growth mode of the potentiostatic electrochemical deposition of Ag on the reconstructed Au (111) electrode surface presented in this work is quite different from those previously reported for the electrochemical deposition on the reconstruction-lifted Au(111) electrode surface and deposition under ultrahigh vacuum (UHV) condition on the reconstructed Au(111) surface, showing the importance of surface structure and electrode potential on the growth mode.

Acknowledgment. The present work was partially supported by a Grant-in-Aid for Scientific Research (A) (2006-2009, No.18205016) and for the Priority Area of "Molecular Nano Dynamics" (2004-2006, No.16072202) from the Ministry of Education, Culture, Sports, Science and Technology (MEXT), Japan.

References and Notes

(1) Hachiya, T.; Itaya, K. *Ultramicroscopy* **1992**, *42*, 445.
(2) Ogaki, K.; Itaya, K. *Electrochim. Acta* **1995**, *40*, 1249.
(3) Chen, C. H.; Vesecky, S. M.; Gewirth, A. *J. Am. Chem. Soc.* **1992**, *114*, 451.
(4) Mrozek, P.; Sung, Y. E.; Han, M.; Gamboa-Aldeco, M.; Wieckowski, A.; Chen, C. H.; Gewirth, A. *Electrochim. Acta* **1995**, *40*, 17.
(5) Garcia, S.; Salinas, D.; Mayer, C.; Schmidt, E.; Staikov, G.; Lorenz, W. J. *Electrochim. Acta* **1998**, *43*, 3007.
(6) Mrozek, P.; Sung, Y. E.; Wieckowski, A. *Surf. Sci.* **1995**, *335*, 44.
(7) Uchida, H.; Miura, M.; Watanabe, M. *J. Electroanal. Chem.* **1995**, *386*, 261.
(8) Corcoran, S. G.; Chakarova, G. S.; Sieradzki, K. *J. Electroanal. Chem.* **1994**, *377*, 85.
(9) Corcoran, S. G.; Chakarova, G. S.; Sieradzki, K. *Phys. Rev. Lett.* **1993**, *71*, 1585.
(10) White, J. H.; Albarelli, M. J.; Abruna, H. D.; Blum, L.; Merloy, O. R.; Samant, M. G.; Borges, G. L.; Gordon, J. G. *J. Phys. Chem.* **1988**, *92*, 4432.
(11) Chabala, E. D.; Ramadan, A. R.; Brunt, T.; Rayment, T. *J. Electroanal. Chem.* **1996**, *412*, 67.
(12) Ramadan, A. R.; Chabala, E. D.; Rayment, T. *Phys. Chem. Chem. Phys.* **1999**, *1*, 1591.
(13) Koos, D. A.; Richmond, G. L. *J. Phys. Chem.* **1992**, *96*, 3770.
(14) Esplandiu, M. J.; Schneeweiss, M. A.; Kolb, D. M. *Phys. Chem. Chem. Phys.* **1999**, *1*, 4847.
(15) Kondo, T.; Morita, J.; Okamura, M.; Saito, T.; Uosaki, K. *J. Electroanal. Chem.* **2002**, *532*, 201.
(16) Borissov, D.; Tsekov, R.; Freyland, W. *J. Phys. Chem. B* **2006**, *110*, 15905.
(17) Dovek, M. M.; Lang, C. A.; Nogami, J.; Quate, C. F. *Phys. Rev. B* **1989**, *40*, 11973.
(18) Chambliss, D. D.; Wilson, R. J. *J. Vac. Sci. Technol. B* **1991**, *9*, 928.
(19) Cercellier, H.; Fagot-Revurat, Y.; Kierren, B.; Malterre, D.; Reinert, F. *Surf. Sci.* **2004**, *566*−*568*, 520.
(20) Didiot, C.; Pons, S.; Kierren, B.; Fagot-Revurat, Y.; Malterre, D. *Surf. Sci.* **2006**, *600*, 3917.
(21) Cercellier, H.; Didiot, C.; Fagot-Revurat, Y.; Kierren, B.; Moreau, L.; Malterre, D. *Phys. Rev. B* **2006**, *73*, 195413.
(22) Maupai, S.; Zhang, Y.; Schmuki, P. *Surf. Sci.* **2003**, *527*, L165.
(23) Tao, N. J.; Pan, J.; Li, Y.; Oden, P. Y.; DeRose, J. A.; Lindsay, S. M.; *Surf. Sci. Lett.* **1992**, *271*, L338.
(24) Allongue, P.; Cagnon, L.; Gomes, C.; Gündel, A.; Costa, V. *Surf. Sci.* **2004**, *557*, 41.
(25) Lay, M. D.; Stickney, J. L. *J. Am. Chem. Soc.* **2003**, *125*, 1352.
(26) Strbac, S.; Magnussen, O. M.; Behm, R. J. *Phys. Rev. Lett.* **1999**, *83*, 3246.
(27) Clavilier, J.; Faure, R.; Guinet, G.; Durand, R. *J. Electroanal. Chem.* **1980**, *107*, 205.
(28) Bulou, H.; Goyhenex, C. *Phys. Rev. B* **2002**, *65*, 045407.
(29) Borensztein, Y.; Lopez-Rios, T.; Vuye, G. *Phys. Rev. B* **1988**, *37*, 6235.